NJC

PAPER
S. T. Hyde *et al.*
Ravels: knot-free but not free. Novel
entanglements of graphs in 3-space
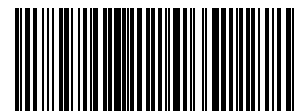
Ravels: knot-free but not free. Novel entanglements of graphs in 3-space

Toen Castle, Myfanwy E. Evans and S. T. Hyde*

Molecular and extended framework materials, from proteins to catenanes and metal–organic frameworks, can assume knotted configurations in their bonding networks (the chemical graph). Indeed, knot theory and structural chemistry have remained closely allied, due to those connections. Here we introduce a new class of graph entanglement: "ravels". These ravels—often chiral—tangle a graph without the presence of knots. Just as knots lie within cycles in the graph, ravels lie in the vicinity of a vertex. We introduce various species of ravels, including fragile ravels, composite ravels and shelled ravels. The role of ravels is examined in the context of finite and infinite graphs—analogous to molecular and extended framework nets—related to the diamond net.

1. Introduction

The bonding networks of molecules, polymers, DNA complexes and extended framework crystals or *nets* (from zeolites to metal–organic frameworks), are all instances of finite and infinite *graphs*. To date, descriptions of these materials as graph embeddings have been largely devoted to two distinct structural approaches: topological and geometric. The former invokes the perspective of graph theory,[1,2] the latter crystallography.[3,4] Physico-chemical characteristics of molecular materials may also depend on spatial features due to the *entanglement* of the graph in space. For example, the electrophoretic mobility of circular DNA has been shown to be sensitive to its knottedness.[5]

Knots, links and more general entanglements lie between the poles of topology and geometry, distinguishing between various threadings of edges within the graph, without regard for the graph geometry. Distinct entanglements may however share a common graph topology (characterised, for example by a connectivity matrix between the graph vertices). Organic chemists are aware of the possibility of entangled or knotted embeddings of finite molecular graphs in 3-space and this has provoked interesting explorations on the part of knot theorists of the role of knotted and linked cycles in molecular chirality.[6–8]

Organic chemists have long pursued the synthesis of knotted synthetic molecules, in response to their connections to molecular chirality as much as their intrinsic beauty.[8–12] Knotted DNA and RNA complexes have also been realized.[13–15] This feature is not limited to biochemical polymers: knotted polymer chains have been synthesised by metal coordination[16] and a theoretical proposal to form knotted polymeric fabrics *via* condensation of monomers on templating surfaces has been presented recently.[17] Multi-stranded and DNA–protein complexes, such as the three-stranded mu protein–DNA complex, adopt a range of entangled guises, whose description and analysis demand a rigorous understanding of embeddings of graphs in 3-space.[18]

The presence of distinct knottings of topologically equivalent nets has been noted in metal–organic frameworks (MOFs).[19,20] The variety of distinct catenation modes of nets in porous frameworks, particularly MOFs, is likely to continue to grow, given the ever-widening range of organic ligands and complexing agents being used in these materials. Taxonomic classification schemata for these catenated graphs have been proposed in the chemical literature.[21–23] Those classifications do not account for subtle entanglement modes, such as ravels.

The identification of distinct entanglements of a given graph is a challenge that has been met in part by exhaustive analyses of knots and links in closed cycles of the graph. The suite of knots and links in a graph affords a useful signature of the graph embedding, as discussed by Kauffman.[24] However, it is incomplete. A full description of entanglement in graphs must go beyond an analysis of cycles, to capture aspects that are not found in closed graphs of degree lower than three (such as the standard degree-two cycles in knots and links).

In this paper we explore an exotic entanglement mode that is possible in both finite and infinite graphs, irrespective of the presence or absence of knots or links. We call these entanglements *ravels*. A ravel can be localised to a vertex, common to three (or more) edges of the graph, just as knots are localised to a cycle. Unlike simpler entanglements, the presence of ravels is not manifested in the collection of standard knots or links contained within the embedded graph, obtainable using the method outlined by Kauffman.[24] These entanglements have been the subject of some analysis among graph theorists, though—to our knowledge—they have not been explored in a systematic manner, and their presence in chemical graphs has remained unexplored. Here we expose these curious objects to further scrutiny.

We first revisit the issue of knotted embedded graphs, and describe their formation by insertion of knots in untangled finite (molecular) and infinite (net) graphs (adamantane and diamond, respectively). We then present a tentative definition

Applied Mathematics Department, Research School of Physical Sciences, Australian National University, Canberra, 0200, Australia. E-mail: stephen.hyde@anu.edu.au

of ravels, based on the possibility of confining them to the neighbourhood of a single vertex in a graph. Next, we describe various types of ravels, based on their *fragility* and their *composite* or *shelled* nature. Lastly, we offer a constructive test for the presence of ravels in embedded graphs. The presence of ravels can only be detected by analysis of specific graphs related to the θ-graph and its higher-degree relatives, bouquet graphs and hybrid graphs of those two classes.

## 2. Nets: topological and geometric descriptions

Consider first the most generic description of a net: the net topology. This depends on the connections between vertices only, rather than details of the linkage geometries. Nets exhibit topological equivalence if there is a graph isomorphism mapping one set of vertices and linkages into the other. This approach is the domain of (topological) graph theory. For example, we can reduce the description of the infinite 3-periodic *diamond* network to a quotient graph, containing distinct vertices for each diamond node within a primitive translational unit cell and edges that denote the connection diagram between distinct vertices. Following Klee, we can label edges by a translation vector that describes the labelled unit cell containing the adjacent vertex, giving a compact symbol that encodes the topology of the extended diamond net in its entirety (Fig. 1).

Delgado Friedrichs and O'Keeffe have shown that this description is often sufficient to deduce a net signature *via* equilibrium placement,[25] using the *Systre* algorithm.[26] For example, we can use the abstract placement to generate a 3-space embedding of the diamond net, by locating vertices at crystallographic coordinates given by the equilibrium placement (barycentric coordinates) within an arbitrary unit cell (*e.g.* a unit cube) and linking vertices by geodesics. Choosing the primitive unit cell of the face-centred cubic lattice gives the familiar tetrahedral embedding of the diamond net in Euclidean 3-space (space group $Fd\bar{3}m$), illustrated in Fig. 2.

It is convenient for our purposes to recognise that this standard geometric embedding of the usual diamond net can be realised as a packing of vertex-shared polyhedra, with additional vertices and edges, in the following manner. First, form a slightly distorted *boracite* net,[4] by linking neighbouring vertices, located at $(\frac{1}{4},\frac{1}{4},\frac{1}{4})$ and $(\frac{1}{2},0,0)$ sites in the $P\bar{4}3m$ space group. Next, add an additional vertex at $(\frac{1}{2},\frac{1}{2},\frac{1}{2})$, and connect to the four nearest degree-3 vertices equivalent to the $(\frac{1}{4},\frac{1}{4},\frac{1}{4})$ site. The resulting net is geometrically congruent to the usual ($Fd\bar{3}m$) diamond net. The distorted boracite net contains a
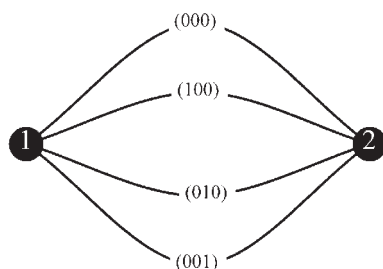
Fig. 1 Labelled quotient graph description of the topological structure of the crystalline *diamond* network.
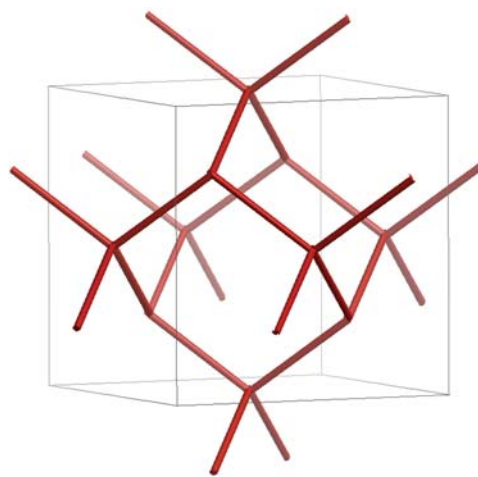
Fig. 2 Symmetric geometric embedding of the untangled *diamond* net in 3-space.

simple cubic array of vertex-shared cages, each bounded by the edges and vertices of the adamantane unit (as in Fig. 3).

3. Entangled nets: knots and links

We define *untangled* graph embeddings of nets to be ambient isotopic to the barycentric embedding produced by the Systre algorithm. In other words: provided a graph embedding can be deformed to a barycentric embedding, *via* the procedure described above without edges passing through each other, the embedding is untangled. This untangled placement is not necessarily free of knots and links, rather it is a defined ground state for the net embedding. (In some cases, barycentric placement fails; we ignore those somewhat (chemically) pathological examples here.)

Proserpio *et al.* have discussed the possibility of distinct embeddings of (*e.g.*) the diamond net, containing threaded cycles that are not found in the standard (untangled) diamond embedding.[19] These *knotted* diamond nets can only be deformed to the usual diamond net by allowing edges to cross through each other. We describe these knotted diamond nets as distinct *isotopes* of the diamond topological net (since they are not deformable into each other *via* an ambient isotopy).

It is useful at this point to describe in brief the concepts of knots and links. A knot is an embedding of a topological cycle in 3-space that is a distinct isotope to the usual (unknotted) loop. Simple knots include the trefoil and cinquefoil, shown in Fig. 4 in the plane with the minimal crossings.

Similarly, links are threadings of multiple cycles, that cannot be disconnected into disjoint components. Links can be described as Brunnian if removal of a single component collapses the link into disjoint cycles (such as the Borromean link, with three component cycles).[27,28] Knot theorists have enumerated knots and links up to limited complexity (minimal crossing numbers and numbers of distinct cycles.)

Nets are more complex than simple cycles, however we can explore some features of entangled nets by analysis of cycles within the net using the standard apparatus of knot theory. Since all crystalline infinite nets (whose vertex degrees exceed two) contain cycles of arbitrarily large lengths (numbers of
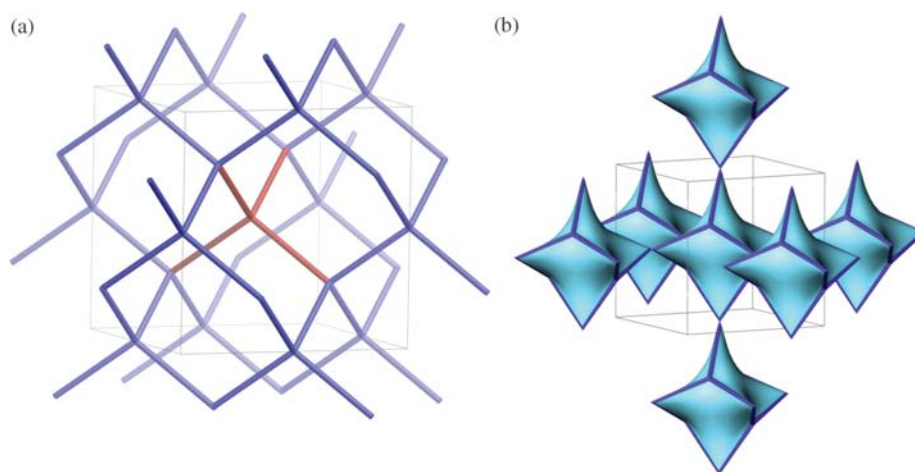
Fig. 3 (a) The diamond net drawn as a distorted boracite net (blue edges) with an interstitial tetrahedral vertex at the body-centre of the cell, linking to nearest degree-3 sites in boracite (red edges). (b) Simple cubic array of 3d adamantane tiles, whose edges form the boracite net (cell origin shifted to body-centre *cf*. (a)). This arrangement combined with a single tetrahedral vertex placed at the unit cell vertices completes the diamond net.
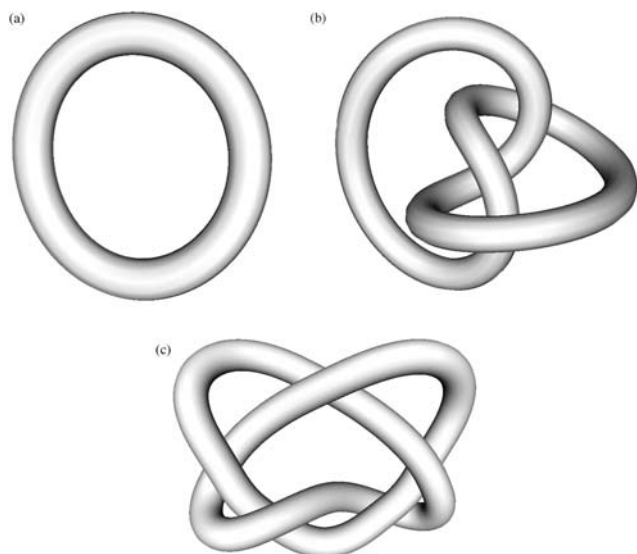

Fig. 4 (a) The trivial knot (or unknot); (b) the trefoil knot and (c) the cinquefoil knot.

vertices), we can detect knots and links of various types within even the simplest nets, classified here as untangled. We may elect to confine analysis of cycle threadings to shortest cycles, such as strong rings of the network.[29] This allows enumeration of threading, *e.g.* as implemented in the *TOPOS* package.[30] This analysis reveals that all (strong ring) cycles in untangled diamond nets contain only trivial knots, with no threading of cycles by edges.

A simple route to construction of knotted nets is *via* entangled polyhedral graph embeddings, stacked to form the infinite net. We have enumerated simpler entangled polyhedra *via* embeddings of polyhedral graphs in the torus (noting that untangled polyhedra embed in the sphere). That enumeration has now been completed for edge graphs of the tetrahedron, octahedron and cube.[31,32]

Among the simpler tangled tetrahedra are two isotopes, containing single trefoil and single cinquefoil knots, illustrated in Fig. 5—we call these embeddings "knotted tetrahedra''. We note in passing that these tetrahedra are chiral.

Addition of degree-two vertices in all edges of the tetrahedron graph gives the edge graph of a single adamantane unit. Adding those vertices to knotted tetrahedral embeddings allows us to build knotted diamond nets, using the recipe illustrated in Fig. 3, where we pack these knotted tetrahedra in a cubic array and add additional tetrahedral vertices. Since the tetrahedra are chiral, many distinct knotted diamond nets can
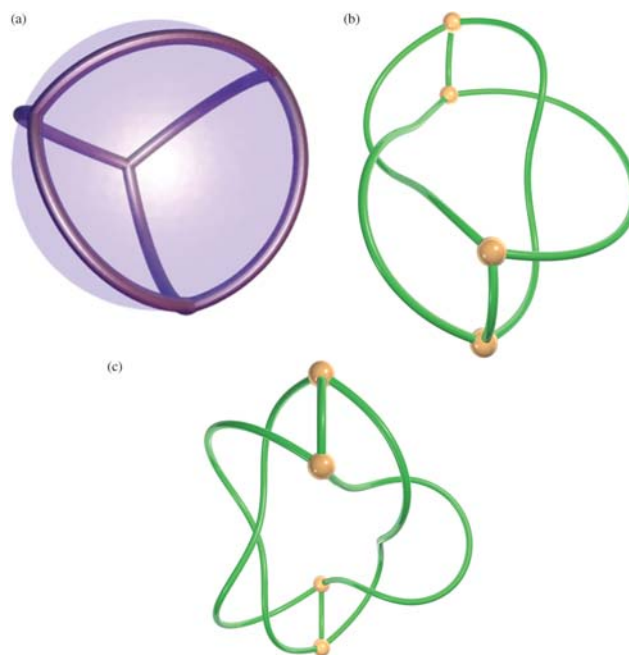
Fig. 5 (a) An untangled tetrahedron graph embedding, lying in a sphere. (b,c) Knotted tetrahedral graph embeddings (in an invisible torus) with cycles forming: (b) a single trefoil and (c) a single cinquefoil knot.
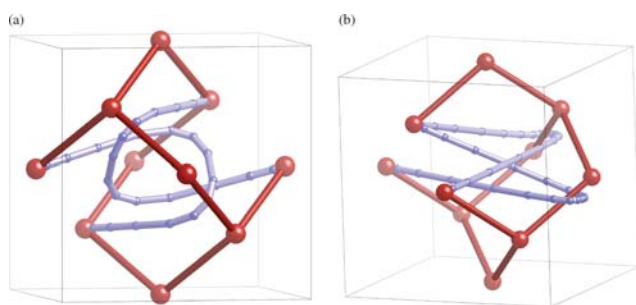
Fig. 6 Fragments of knotted diamond nets formed by stacking knotted tetrahedra as shown in Fig. 5: (a) trefoil diamond and (b) cinquefoil diamond. The edges that generate distinct diamond isotopes are coloured blue; edges that are unchanged from the untangled diamond isotope are coloured red.

be generated by combining enantiomers of distinct knotted tetrahedra. We illustrate just two of the simpler examples, containing trefoils and cinquefoils only (and links) in Fig. 6.
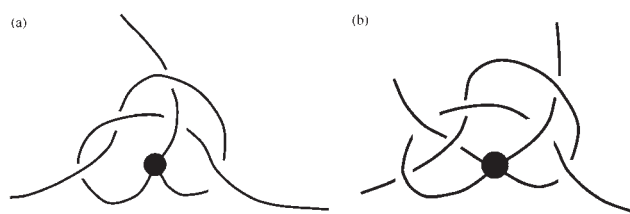
4. Ravels

In the course of our analysis of entangled polyhedra, we have come across a novel mode of edge entanglement that we call *ravels*. Consider the entanglement shown in Fig. 7. It can be seen that the closure of any pair of edges results in an unknotted cycle. The presence of one vertex common to all cycles prevents there being any disjoint cycles, and hence rules out the occurrence of links. Despite the absence of knots and links, the arrangement can be seen to be entangled, since 'pulling' on the edges does not straighten the structure out to a trivial star-shaped arrangement. We call such non-trivial entanglements around a vertex with no knots and links *ravels*.

Ravels are defined as a local phenomenon around vertices of degree three or larger, and are formed by the mutual weaving of the edges emerging from a single vertex. We call ravels composed of *n* edges coincident to a vertex *n-ravels*. Since the entanglement is due to the mutual weaving of the edges rather than knotting or pairwise interlinking, ravels are reminiscent of Brunnian links.

Exposition of the variety of ravels is at least as complex as knot and link enumeration. For example, the most efficient
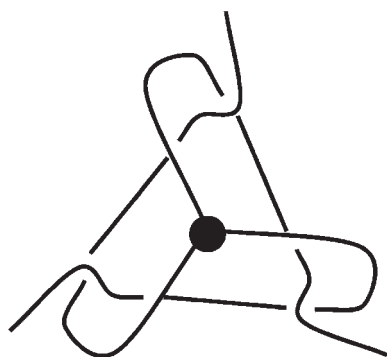
Fig. 8 Simple non-trivial (a) 3- and (b) 4-ravels drawn with minimal crossing numbers (5 and 7, respectively).

presentation of the simplest 3-ravel contains 5 crossings in a planar diagram, compared with a minimal crossing number of just 3 for the smallest knot (the trefoil). Some examples of ravels are shown in Fig. 8.

A ravel is defined to be *universal* when the closure of all 'dangling ends' of the neighbourhood of the ravel at a common second vertex remains free of knots and links. The graph topology of this closure of *n* strands at a common second vertex is called a θ_n ravel, from the shape of the Greek letter θ for the closure of a 3-ravel. Presentations of simple universal ravels of degrees 3, 4 and 5 are shown in Fig. 9. The figure includes the analogous entanglement of a degree-2 configuration: a trefoil knot. We can therefore view ravels as 'branched knots'.
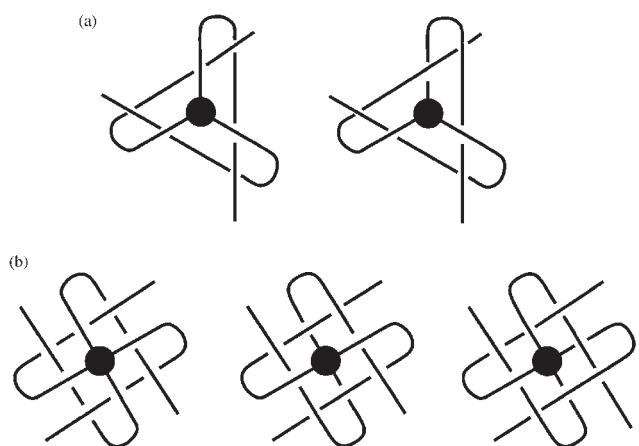
Examples of universal 3- and 4-ravels, excluding their chiral enantiomers, are shown in Fig. 10.

Examples of a θ_3- and a θ_4-graph embedding, containing universal 3- and 4-ravels, respectively, with the loose strands fused at a second vertex, are shown in Fig. 11.
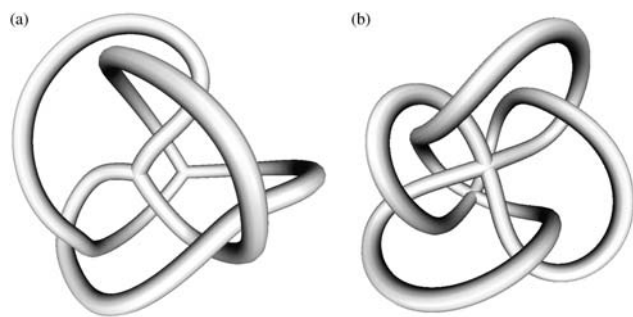
A wider class of ravels involves the incomplete closure of the ravelled strands. If there exists a closure of a ravel in which each dangling strand can be connected with at least one other strand without inducing knotting or linking, then the ravel is *selective*. This contrasts with universal ravels in which *all* strands close by connecting to a single vertex, and hence each
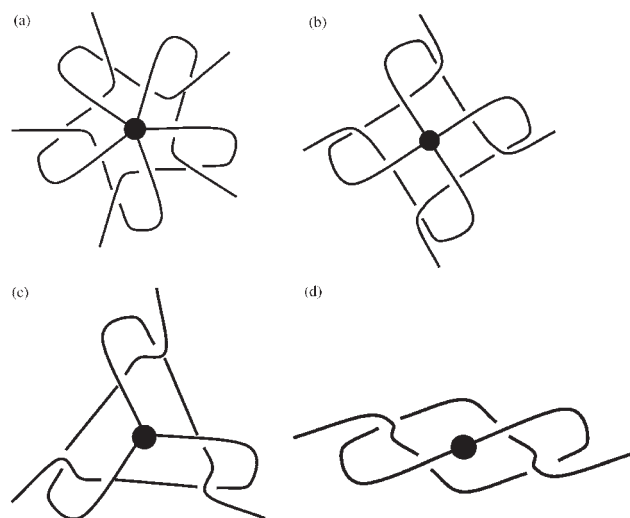
Fig. 9 Universal *n*-ravels in the vicinity of vertices of (a) degree five, (b) four and (c) three. (d) The degree-two analogue is a trefoil knot. Tightening the two loose ends of the trefoil knots the configuration; tightening the 3, 4 or 5 loose edges of the ravels entangles the structures, though knots are not formed.

Fig. 7 A symmetric representation of the simplest ravelled entanglement. Despite this structure being distinct from a trivial vertex, replacing a standard degree-3 vertex with this entangled node creates no new knots or links in a graph embedding.

Fig. 10 Distinct universal 3- and 4-ravels, excluding chiral enantiomers.

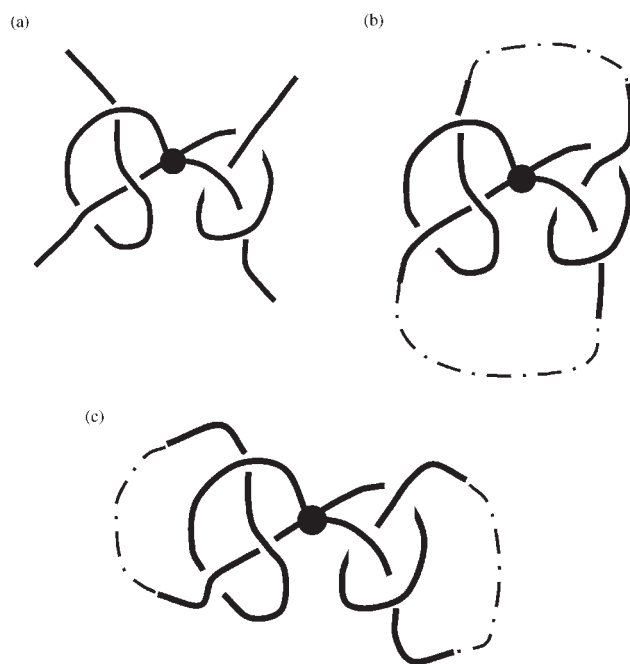**Fig. 11** Examples of universal (a) 3- and (b) 4-ravels in embeddings of the θ_3-graph and the θ_4-graph (see Fig. 14), corresponding to the universal 3- and 4-ravels illustrated in Fig. 9.

Fig. 12 (a) A selective 4-ravel whose insertion into a graph depends on the strand closure mode. Pairing distinct strands gives an entangled but unknotted bouquet graph (b) or a bouquet graph with a pair of trefoils (c).

Fig. 13 Embeddings of (a) degree-4 and (b) degree-6 (right) bouquet graphs that are unknotted, unlinked and ravelled. A planar presentation of the degree-4 example is shown in Fig. 12(b) while the degree 6 example is topologically equivalent to the bottom right-hand image of Fig. 14.
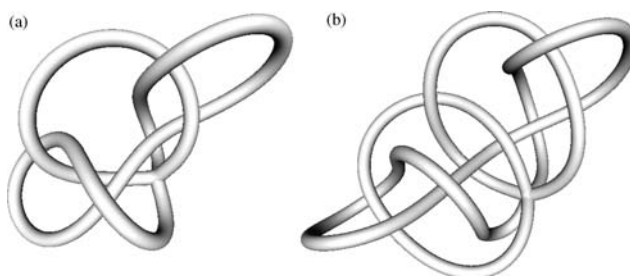
other. Note that universal ravels are a subset of selective ravels.

Selective ravels are more restricted in the manner in which they can be involved in graph embeddings, as only certain edge gluings allow the resulting graph to remain entangled without the presence of additional knots induced by the ravelled vertex. For example, the 4-stranded ravel illustrated in Fig. 12 can close to form either entangled but unknotted embeddings, or knotted embeddings. These particular closures of strands, forming lobes sharing a common central vertex, results in the graph topology known as *bouquet* graphs. Provided the vertex has even degree (≥ 4), some selective ravels may close into a bouquet graph. Examples for degree-4 and -6 vertices are shown in Fig. 13. The degree-4 example contains the (likely) minimal 6-crossing selective 4-ravel with ends merged as shown in Fig. 12(b).

Ravels are able to be contained in a ball enclosing a graph vertex. Their entanglement type, however, may depend on loops containing those edges beyond the ball, or the edge closure. A star of edges can close in a number of distinct ways, as shown in Fig. 14. By definition, universal n-ravels are entangled regardless of the closure of the edges; we are therefore free to analyse universal n-ravel entanglements by replacing one node of a θ_n-graph by the universal ravel. On the other hand, the entanglement or otherwise of selective ravels

depends on the edge closure, in which case distinct closure graphs give distinct entanglements.

5. Properties of ravels

The removal of a single edge from the ravels shown in Fig. 7–9 leads to the demise of the entire ravel. In these cases, the interdependency created by the mutual weaving of the edges of the ravel makes every edge essential to the entanglement. These are *fragile* ravels.

More complex ravels can be composed out of combinations of smaller ravels. This composition can take the form of edge-contraction, where a single edge of one ravel is identified with a single edge of another ravel, then the edge is contracted such that the vertices of the two ravels become one. This process is reversible, so *composite ravels* may be decomposed into
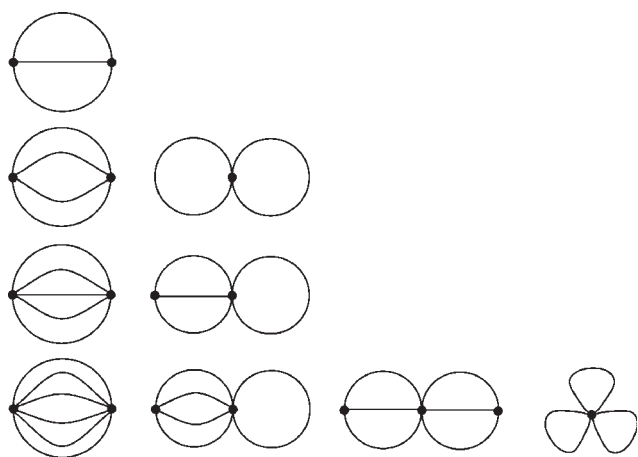
Fig. 14 Topological graphs that admit ravelled entanglements. 3-, 4-, 5- and 6-ravelled graphs are in successive rows. The leftmost images are the generalised θ_n-graphs, which are the closures of universal ravels. The other images correspond to the possible distinct closures of selective ravels. The presence of these graphs within embedded graphs leads to the possibility of unknotted and unlinked entanglements within those graphs.

simpler ravels. An example of a composite ravel is shown in Fig. 15. Ravels composed in such a way are not fragile, as the removal of an edge will reduce at most one of the two component ravels of the composite ravel to a trivial (un)ravel.
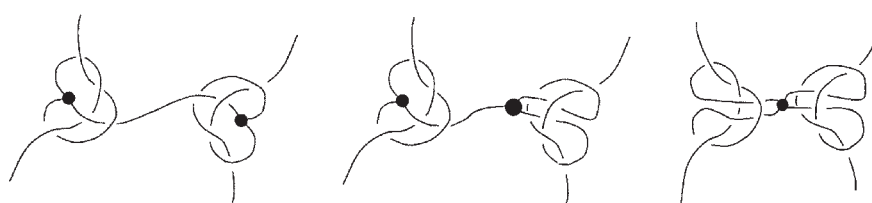
Ravels can also be combined by gluing strands: a connect-sum operation that can be done repeatedly to give chains or networks of ravels. An alternative form of connect-summing is to build them in concentric shells around each other, as shown in Fig. 16. These *shelled ravels* are constructed by replacing the immediate neighbourhood of a vertex at the centre of a ravel with a second ravel of the same degree. If each of the component ravels is fragile, then the composed shell ravel will also be fragile, as each shell will disentangle with the removal of an edge.

We note that the entanglement of composed ravels depends on details that remain to be explored in detail, though some results are canvassed in section 9. For example, shelled ravels may give an untangled configuration.
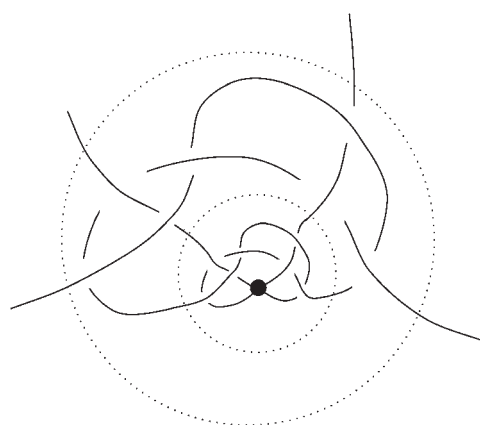
6. Entangled nets

Since the introduction of ravelled vertices does not create new knots or links within graph embeddings, they can be introduced at will into finite or infinite nets, without modifying the knotted or linked character of the net. Evidently ravels, knots and links can coexist in an embedded (and entangled) net.
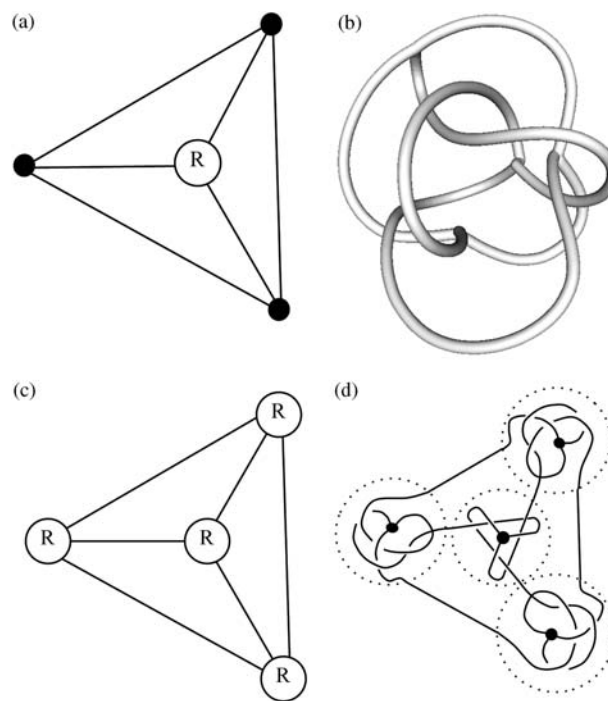
Fig. 17 shows how 3-ravels may be introduced into the structure of a finite graph, here a tetrahedron. As ravels may

Fig. 16 Composition of two concentric ravels, forming a shelled ravel.

Fig. 17 (a,b) An unknotted, ravelled tetrahedron formed by replacing a single vertex by a 3-ravel (marked *R*). A schematic view is shown in (a), (b) shows a specific example, whose ravel is the universal 3-ravel, shown in Fig. 9(c). (c) A ravelled tetrahedron with ravels located at all vertices. (d) Chiral ravelled, knot-free tetrahedron with all vertices containing universal 3-ravels. Compare these images with those in Fig. 5.

Fig. 15 A composite ravel formed by gluing a pair of ravels (fusing a strand in each) followed by edge contraction.

be chiral, the introduction of ravels into an otherwise achiral structure can result in the complete structure being either chiral or achiral, depending on the location of the ravels.

Because ravels are local to a vertex, they can be introduced to unravelled embeddings by the following local operation. First, remove a small ball enclosing a vertex and edges from the graph by cutting the edges in the vicinity of the vertex. Then thread the strands (*e.g.* as in Fig. 7), with each strand end returning to its original position on the surface of the ball. Finally, reposition the ball in its original location in the graph and rejoin the edges, giving a ravelled vertex. We can form a ravelled tetrahedron graph by replacing all degree-3 vertices by a universal 3-ravel, using this procedure. The 3-ravelled tetrahedon can then be used to construct a simple 3-ravelled example of the diamond net as follows. Insert a degree-2 vertex in each edge of the tetrahedral graph; the new structure is topologically equivalent to adamantane Fig. 18(a). The ravelled adamantane that results is shown in Fig. 18(b).

A distinct ravelled diamond network can be constructed by replacing each of the degree-4 diamond vertices with a universal 4-ravel, such as that in Fig. 9(b), illustrated schematically in

Fig. 18(c). This produces the partially ravelled diamond shown in Fig. 18(d).

7. Detection of ravels in an embedded graph

So far, we have described the formation of an entangled graph by replacement of graph vertices with ravels. But what of the inverse problem: the detection of ravels in a graph? We sketch a constructive solution in this section, involving subgraphs of the embedded graph. Graph theory defines the (topological or embedded) subgraph of a graph, G, to be a graph that results by deleting edges of G and retaining all vertices on conserved edges.

Since we seek vertex-localised entanglements, we first extract the embedded subgraph consisting of all edges of topological length unity from the vertex v. In other words, delete all elements of the embedded graph except those edges radiating from v, to the nearest neighbouring vertices w_i (where $i \in \{1,z\}$ and the degree of vertex $v = z$). The entanglement of any given ravel depends upon the closure of strands beyond the vertex of interest. For example, selective ravels placed in bouquet graphs may be ambient isotopic
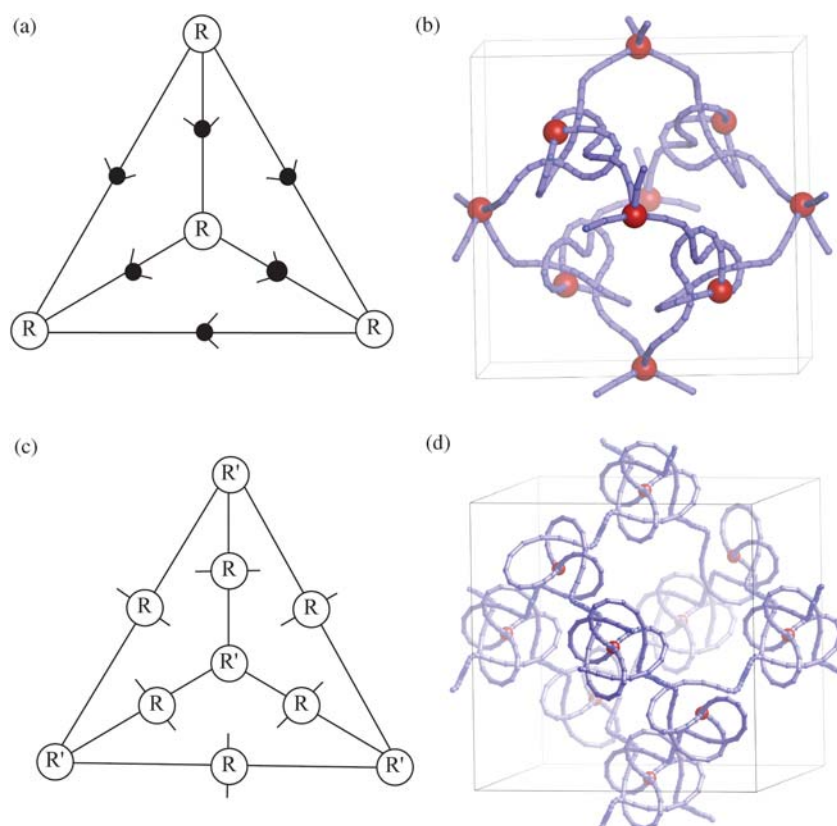
Fig. 18 (a) Schematic diagram of an adamantane cage within the diamond net, with ravels at degree-3 vertices, related to a ravelled tetrahedron (*cf*. Fig. 17(c)). Open circles (marked R) mark degree-3 ravel locations; filled dots mark degree-4 vertices, located at the degree-2 kinks of the adamantane cage. This fragment of the infinite diamond net is entangled, but unknotted. (b) The corresponding fragment of the diamond net, with universal 3-ravels inserted at the four degree-3 vertices as in (a), (*cf*. Fig. 17(d)). (c) Alternative ravelled configuration to (a), with all degree-4 vertices of the adamantane fragment of the diamond net containing universal 4-ravels (marked R), while the degree-3 vertices are replaced by 3 strands of universal degree-4 ravels (*cf*. Fig. 9(b), marked R'). Since the universal 4-ravel is fragile, the degree-3 vertices untangle. (d) Embedding of (c). In contrast to (b), this fragment is (partially) untangled at the degree-3 vertices. However, if additional strands are woven into the degree-3 vertices, completing 4 strands of the 4-ravel, a ravelled diamond net results.

to the untangled bouquet graph embedding—each lobe may be able to disentangle with the others, see, for example Fig. 12. It is thus necessary to determine which pairs of strands have a cycle closure in the graph.

Closure of the star of edges, forming wheel graphs, or subgraphs thereof, are constructed by grouping the perimeter vertices w_i into k equivalence classes. Elements of each class are linked by 'rim sectors', made up of edges of the embedded graph that do not pass through v and contain the smallest number of vertices of all possible (v-avoiding) paths connecting the rim vertices in the jth equivalence class, w_{ij}. In this way, we form a "flower" graph with k lobes, $B^k(v)$, whose form resembles one of the graphs in Fig. 14 (possibly generalised to higher degree). The spatial embedding of the edges and of the subgraph, $B^k(v)$, is equivalent to the corresponding edges of the original embedded graph, G, whose edges form the spokes and rim sectors of $B^k(v)$.

Note that there may be more than a single flower graph centred on the same vertex, v. This can arise in two ways. First, there may be more than one shortest rim sector in the graph. Second, there may be more than one decomposition into equivalence classes, due to multiple (more than two) rim edges from a given spoke vertex, bridging the spoke vertex to (more than two) distinct spoke vertices. Nevertheless, the collection of flower graphs is finite, assuming the parent graph's vertices are all of finite degree. The construction must be applied to all vertices v in the graph.

The embedding of these flower graphs can then be characterised, for example, by the Yamada polynomial, which distinguishes graph embeddings using similar techniques to better-known polynomial invariants for knots and links.[33] This polynomial provides a structural invariant: if the polynomial is distinct from that of the untangled (*i.e.* planar) embedding and knotted embeddings, the net potentially contains a ravel. We can determine the Yamada polynomials for various ravels within flower graphs, generating a look-up table to search for ravels in the graph. Unequivocal evidence for the ravel requires comparison of the flower graph Yamada polynomial with those of known ravelled flower graphs.

The ravel entanglement can be further understood by considering any sub-ravels it contains. This is done by selectively deleting edges from the flower graph—equivalent to removing strands from the ravel. Each resulting subgraph embedding can be analysed in the same way as the parent ravel, and provides information about the fragility or composite character of the ravel. In this way, for example, a 4-ravel which is composed of a 3-strand ravel plus an extra unwoven strand can be identified.

8. Discussion

We have introduced here an entanglement mode in embedded graphs—ravels—that is not captured by simple knot or link analyses. The presence of ravels demonstrates the incompleteness of topological invariants of entangled graphs, which characterise the graph embedding in terms of its knots and links alone[24]—since ravels do not contain knots or links, their presence in nets cannot be detected by cycle analysis. To find entanglements beyond knots and links, flower sub-graphs must be searched, as outlined above.

After this work was completed, we found that these entanglements have been noted before. To our knowledge, the first recognition of ravels is due to Kinoshita, who presented an embedding of the θ-graph containing a simple 3-ravel, ambient isotopic to that of Fig. 11.[34] This example was proven by Wolcott to be chiral, who also presented a triply-infinite family of related entangled θ-graph embeddings, also knot-free.[35,36] Later, Suzuki presented a family of simple ravelled modes of generalised θ-graphs of arbitrary degree n (θ_n-graphs, *cf.* Fig. 11).[37] In a later enumeration of θ-graph embeddings, Moriuchi lists 5-, 7- and 9-crossing examples, all free of knots or links;[38] those examples correspond to ravels. Wolcott and Simon have constructed links associated with ravels (or, in their language, 'minimally knotted graphs') that prove entanglement;[39] more specific invariants for ravelled θ-graphs have also been reported.[40]

A number of methods to 'glue' ravels, forming more complex ravels, have been canvassed in section 6. Some of those have also been analysed elsewhere. The connect-sum technique is shown to have a prime decomposition by Suzuki. A subset of shelled ravels has been discussed by Wolcott, who considered generalised connect-sums, and showed that degree-3 connect-sums of ravels always produce a ravel,[36] whereas connect-sums between ravels and untangled graphs can form either ravels or untangled graphs.

Beautiful though this topic is, it is fair to question its relevance to the chemical realm. First, ravelled structures offer a tantalising new class of chiral finite graphs that offer a substantial challenge to the organic synthetic chemist, akin to the syntheses of knotted organic species.[11–15] For example, can the simplest examples, shown in Fig. 11 and 13, be realised as molecules? However, the implications of ravels go beyond that challenge. In our view, ravels may well be found in extended molecular frameworks with flexible polymeric links, such as metal organic frameworks, in the future. Lastly, consideration of knotting in biochemical graphs, including proteins and DNA–protein complexes, must be extended to the broader class of entanglements, including knots, links and ravels.

References

1 W. Klee, *Cryst. Res. Technol.*, 2004, **39**, 959–968.
2 J.-G. Eon, *Acta Crystallogr., Sect. A*, 2005, **61**, 501–511.
3 M. O'Keeffe and B. Hyde, *Crystal Structures. 1. Patterns and Symmetry*, Mineralogical Society of America, Washington, 1996.
4 M. O'Keeffe, *Reticular Chemistry Structural Resource*, 2003, Available at http://rcsr.anu.edu.au.

5 S. Trigueros, J. Arsuaga, M. Vazquez, D. Sumners and J. Roca, *Nucleic Acids Res.*, 2001, **29**, e67.

6 J. Simon, *J. Comput. Chem.*, 1987, **8**, 718–726.

7 J. Simon, in *Graph Theory and Topology in Chemistry*, Elsevier, Amsterdam, 1987, ch. A topological approach to the stereochemistry of nonrigid molecules, pp. 43–75.

8 E. Flapan, *When Topology Meets Chemistry: A Look at Molecular Chirality*, Cambridge University Press, Cambridge, 2000.

9 D. Walba, in *Graph Theory and Topology in Chemistry*, Elsevier, Amsterdam, 1987, ch. Topological stereochemistry: Knot theory of molecular graphs, pp. 23–42.

10 C. Liang and K. Mislow, *J. Math. Chem.*, 1994, **15**, 1–34.

11 C. Dietrich-Buchecker and J.-P. Sauvage, *Chem. Rev.*, 1987, **87**, 795–810.

12 C. Dietrich-Buchecker and J.-P. Sauvage, *New J. Chem.*, 1992, **16**, 277–285.

13 J. E. Mueller, S. M. Du and N. C. Seeman, *J. Am. Chem. Soc.*, 1991, **113**, 6306–6308.

14 N. C. Seeman, J. Chen, S. M. Du, J. E. Mueller, Y. Zhang, T.-J. Fu, Y. Wang, H. Wang, S. Zhang, C.-S. T. Soumpasis, A. H.-J. Wang and V. B. Zhurkin, *New J. Chem.*, 1993, **17**, 739.

15 O. Safarowsky, M. Nieger, R. Fröhlich and F. Vögtle, *Angew. Chem., Int. Ed.*, 2000, **39**, 1616–1618.

16 H. Adams, E. Ashworth, G. Breault, J. Guo, C. A. Hunter and P. C. Mayers, *Nature*, 2001, **411**, 763.

17 D. Andrae, *New J. Chem.*, 2006, **30**, 873–882.

18 I. Darcy, J. Luecke and M. Vazquez, *Algebraic Geometric Topology*, 2007, submitted.

19 L. Carlucci, G. Ciani and D. M. Proserpio, *CrystEngComm*, 2003, **5**, 269–279.

20 L. Carlucci, G. Ciani and D. M. Proserpio, *Coord. Chem. Rev.*, 2003, **246**, 247–289.

21 S. Batten and R. Robson, *Angew. Chem., Int. Ed.*, 1998, **110**, 1460–1494.

22 S. Batten, *CrystEngComm*, 2001, **3**, 67–73.

23 V. Blatov, L. Carlucci, G. Ciani and D. Proserpio, *CrystEngComm*, 2004, **6**, 377–395.

24 L. H. Kauffman, *Trans. Am. Math. Soc.*, 1989, **311**, 697–710.

25 O. Delgado-Friedrichs, M. O'Keeffe and O. M. Yaghi, *Acta Crystallogr., Sect. A*, 2003, **59**, 351–360.

26 O. D. Friedrichs, *Generation, Analysis and Visualization of Reticular Ornaments using* GAVROG, available at http://www.gavrog.org/.

27 H. Brunn, *S.-B. Math.-Phys. Kl. Bayer Akad. Wiss.*, 1892, **22**, 77–99.

28 C. Liang and K. Mislow, *J. Math. Chem.*, 1994, **16**, 27–35.

29 O. D. Friedrichs and M. O'Keeffe, *Acta Crystallogr, Sect. A*, 2003, **59**, 22–27.

30 V. Blatov, *IUCr CompComm Newslett.*, 2006, **7**, 4–38.

31 S. Hyde and G. Schröder-Turk, *Acta Crystallogr, Sect. A*, 2007, **63**, 186–197.

32 T. Castle, V. Robins and S. Hyde, in preparation.

33 L. S. Yamada, *J. Graph Theory*, 1989, **13**, 537–551.

34 S. Kinoshita, *Pac. J. Math.*, 1972, **42**, 89–98.

35 In common with other authors, Wolcott describes all entangled graph embeddings as 'knotted', even if they are knot-free. We prefer to describe knot-free embedded graphs that are not isotopic to their simplest (unentangled) embedding in the sphere as 'entangled'.

36 K. Wolcott, in *Geometry and Topology: Manifolds, Varieties, and Knots*, Marcel Dekker, New York, 1987, ch. The knotting of theta curves and other graphs in S^3, pp. 325–346.

37 S. Suzuki, *Kobe J. Math.*, 1984, **1**, 19–22.

38 H. Moriuchi, available at knot.kaist.ac.kr/2004/proceedings.php.

39 J. K. Simon and K. Wolcott, *Topology Appl.*, 1990, **37**, 163–180.

40 L. Kauffman, J. Simon, K. Wolcott and P. Zhao, *Topology Appl.*, 1993, **49**, 193–216.

41 R. Scharein, *KnotPlot*, Available at http://knotplot.com/.